Int. J. Heat Mass Transfer. Vol. 22, pp. 27–38
Pergamon Press Ltd. 1979. Printed in Great Britain

A THEORETICAL ANALYSIS OF EVAPORATING DROPLETS IN AN IMMISCIBLE LIQUID

M. R. MOKHTARZADEH* and A. A. EL-SHIRBINI
Mechanical Engineering Department, Imperial College of Science and Technology, London, SW7 2BX, England

(*Received* 15 *March* 1978)

Abstract—This paper presents a theoretical analysis of the evaporation of a single droplet during its rise in a column of an immiscible liquid. Governing equations are derived then solved simultaneously applying a numerical method. Results are presented for two combinations: butane/distilled water and pentane/distilled water. The model was examined for different initial droplet sizes, temperature differences, initial velocities and initial temperatures. The predicted results are compared with experimental results of previous workers.

NOMENCLATURE

C_D, drag coefficient;
C_p, specific heat [J/kg K];
D, equivalent spherical diameter of bubble-droplet [m];
d, equivalent spherical diameter of initial droplet [m];
g, standard gravitational acceleration [m/s^2];
hH, instantaneous heat-transfer coefficient [J/s m^2 K];
h_{fg}, heat of vaporization [J/kg];
k, heat conductivity [J/s m K];
m, unevaporated mass of liquid in the bubble-droplet [kg];
m_{00}, initial mass of droplet [kg];
P, vaporization pressure of the dispersed phase [N/m^2];
$\bar{P}$, mean pressure [N/m^2];
$P_{s\infty}$, pressure far from the bubble-droplet [N/m^2];
P_c, continuous-phase liquid pressure [N/m^2];
R, radius of bubble-droplet [m];
T, vaporization temperature of the dispersed phase [°C];
T_c, temperature of the continuous phase [°C];
t, time [s];
U, rise velocity of bubble-droplet [m/s];
v, velocity [m/s];
V, volume [m^3];
Z, height [m];
z, vertical axis;
X, growth rate [m/s];
ΔT, temperature difference, $\Delta T = T_c - T$ [°C];
Nu, Nusselt number, $Nu = hD/k$;
Re, Reynolds number, $Re = \rho UD/\mu$;
Pr, Prandtl number, $Pr = \mu C_p/k$;
Pe, Peclet number, $Pe = Re \times Pr$;
r, θ, ψ, spherical coordinates.

Greek symbols

ϕ, velocity potential;
ρ, density [kg/m^3];
σ, interfacial tension [N/m];
μ, viscosity [kg/m s];
ξ, vaporization ratio, $\xi = 1 - m/m_{00}$.

Subscripts

c, continuous phase;
d, droplet;
f, time of complete evaporation;
l, dispersed phase;
0, reference point, $t = 0$;
v, vapour.

1. INTRODUCTION

DESALINATION of sea water by freezing has some advantages when compared with other desalination processes [1,2]. However, this method needs more understanding to be made economically viable. Considerable research in this field has been supported by the Office of Saline Water,† United States Department of the Interior (e.g. [3,4]). Refrigeration is carried out by injecting an immiscible-low-boiling-point refrigerant in water which is contained in a freezer unit. Evaporation of the injected liquid causes the other liquid to cool. Among earlier investigations are those which are reported by Klipstein [5] and by other workers [6–23].

2. DESCRIPTION OF THE PROBLEM

Consider a single droplet which is injected into another immiscible liquid. If the droplet is at saturation temperature corresponding to its pressure and in the meantime is cooler than the surrounding medium, the droplet should evaporate. However, start of evaporation needs the presence of a tiny nucleus of gas or vapour, otherwise droplet superheat may occur. Mechanisms of bubble nucleation of superheated drops in other liquids are discussed by

* Ph.D. Research student.
† Now the Office of Water Research and Technology.

Moore *et al.* [24] and Jarvis *et al.* [25]. Boiling modes of superheated drops in an immiscible liquid are examined by Mori *et al.* [26, 27] using high speed photography. Nucleation was set by small bubbles of nitrogen [16], air [3, 11, 22] or electrically [5, 19]. Depending on the values of interfacial tensions, i.e. continuous phase-droplet; continuous phase-vapour and surface tension of liquid droplet, the bubble may be expelled into the surrounding liquid or remain within the droplet boundary [24]. Gradon and Selecki [15, 21] discuss the importance of the surface tensions of both liquids, which causes two completely different mechanisms of evaporation. If the surface tension of the continuous phase is higher than the surface tension of the droplet and the average density of the bubble-droplet is smaller than the density of the continuous phase, the growing bubble-droplet will move upwards with vapour accumulating at the top of the liquid. Thus, the process starts with a droplet and ends with a bubble. The problem is completely neither of bubble nor of droplet nature. But as it is clear from photographic evidence [6] when 1% of the mass of the droplet is evaporated, most of the bubble-droplet system is occupied with vapour. Thus, during most parts of the evaporation process, the system behaves more like a bubble than a droplet. Depending on the initial size of the droplet, the growing bubble-droplet may have different shapes like a sphere, an ellipsoid or cap shape.

Evaporation time of a droplet is mainly dependent on the size of the initial droplet and temperature difference between the two liquids [6].

Studies on the heat-transfer coefficients to evaporating droplets has been done theoretically (e.g. [6, 18, 23]) and experimentally (e.g. [6, 11–14, 16, 23]) by previous workers. Simpson *et al.* [17] reported that a droplet oscillated from side to side and this caused the unevaporated liquid to slosh or swing from side to side. They based their theory [18] on this observation and by assuming that the oscillating liquid butane forms a film on the inside surface of the bubble. Heat-transfer coefficients may be calculated from a knowledge of the change of volume of bubble-droplet system. Determination of the bubble-droplet volume was done photographically (e.g. [6, 11, 16]) and by using a dilatometric method [12, 14, 23]. Prakash *et al.* [11] mentioned that measurements of the volume of the bubble-droplet photographically were only reliable up to 10% evaporation. Dilatometric method is reported to be more advantageous than the photographic method [14].

Rise velocity of the bubble-droplet varies during the whole process. An increase of velocity after 0.1% evaporation is reported by Sideman *et al.* [6]. Simpson *et al.* [17] reported a nearly constant velocity of butane bubble-droplets in water up to a diameter ratio 2.7 and 2.0 in brine. Afterwards the velocity increased. Motion of an evaporating droplet in an immiscible liquid has been studied theoretically and experimentally by Selecki *et al.* [20].

3. THEORETICAL MODEL

3.1. *Assumptions*

(a) Single bubble-droplet system. (b) The system boundary is spherical. (c) The surrounding liquid has a constant temperature throughout, incompressible, infinite in extent and quiescent. (d) The system boundary is impermeable to substance but permeable to heat. (e) Both liquids are pure. (f) Movement of the bubble-droplet during its ascent is rectilinear.

3.2. *Coordinate system*

The coordinate system moves with the bubble-droplet and its origin is located at the centre of sphere, Fig. 1. Because of assumption (b), the flow around the system is axisymmetric and every point in the field can be specified by r, θ and t. The position of the centre of sphere is specified by Z which is a function of time.

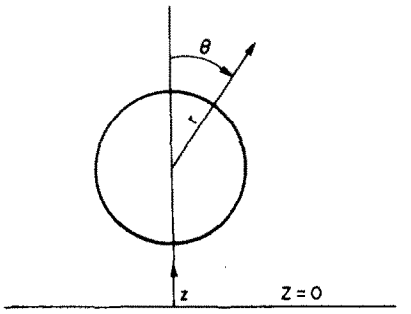

FIG. 1. Coordinate system.

3.3. *Governing equations*

3.3.1. *Momentum equation.* Assuming non-viscous flow, neglecting the viscosity term in the equation of motion (Navier–Stokes), we get:

$$\rho\left[\frac{\partial v}{\partial t}+(v\cdot\nabla v)\right]=-\nabla P_c+\rho g. \tag{1}$$

If it is further assumed that the flow around the system is potential flow, the velocity can be obtained as:

$$v=-\nabla\phi \tag{2}$$

where: $\phi=\phi(r,\theta,t)$.

Applying continuity equation, the velocity potential must satisfy Laplace equation:

$$\nabla^2\phi=0. \tag{3}$$

Equation (3) can be solved for an expanding and translating boundary motion separately and superposition of the two solutions gives the solution for the simultaneous motions.

Boundary conditions for the expanding boundary are:

$$\left.\begin{array}{ll} 0\leqslant\theta\leqslant 2\pi, & v_\theta=0 \\ \begin{cases} r=R \\ 0\leqslant\theta\leqslant 2\pi, \end{cases} & v_r=\dfrac{\mathrm{d}R}{\mathrm{d}t} \\ r\to\infty, & v\to 0 \end{array}\right\} \tag{4}$$

Using boundary conditions (4), solution of equation (3) for an expanding spherical boundary is:

$$\phi_1(r,t) = \frac{R^2}{r}\frac{dR}{dt}. \tag{5}$$

For a translating spherical boundary, the boundary conditions are:

$$\left.\begin{array}{lll} \text{at } r = R & v_r = U\cos\theta & \\ & v_\theta = -U\sin\theta & \\ r \to \infty & v \to 0 & \end{array}\right\} \tag{6}$$

where U is the rise velocity of the system. Using boundary conditions (6), solution of equation (3) for a translating spherical boundary is:

$$\phi_2(r,\theta,t) = \frac{1}{2}U\frac{R^3}{r^2}\cos\theta. \tag{7}$$

Superposition of solutions (5) and (7) yields:

$$\phi(r,\theta,t) = \frac{R^2}{r}\frac{dR}{dt} + \frac{1}{2}U\frac{R^3}{r^2}\cos\theta \tag{8}$$

which is potential flow field around a translating and expanding spherical boundary in quiscent medium.

Using equation (2) in (1), we get:

$$\nabla\left[-\frac{\partial\phi}{\partial t} + \frac{v^2}{2} + \frac{P_c}{\rho}\right] = g. \tag{9}$$

Using the following boundary conditions:

$$\left.\begin{array}{ll} \text{at } r \to \infty & P_c \to P_{s\infty} \\ & v \to 0 \end{array}\right\} \tag{10}$$

where $P_{s\infty}$ is pressure far from the bubble-droplet and is equal to the hydrostatic pressure at the bubble-droplet level. Integration of equation (9) yields:

$$-\frac{\partial\phi}{\partial t} + \frac{v^2}{2} + \frac{P_c - P_{s\infty}}{\rho} = 0. \tag{11}$$

Since the coordinate system is moving [28]:

$$\left.\begin{array}{l} \dfrac{dr}{dt} = -U\cos\theta \\ \dfrac{d\theta}{dt} = \dfrac{U}{r}\sin\theta. \end{array}\right\} \tag{12}$$

At $r = R$, substituting velocity components v_r and v_θ in equation (11) and differentiation of equation (8), we obtain:

$$\frac{P_c - P_{s\infty}}{\rho} = R\frac{d^2R}{dt^2} + \frac{3}{2}\left(\frac{dR}{dt}\right)^2 + \frac{3}{2}U\frac{dR}{dt}\cos\theta + \frac{1}{2}R\frac{dU}{dt}\cos\theta + \frac{U^2}{2}\left(1 - \frac{9}{4}\sin^2\theta\right). \tag{13}$$

The mean pressure around the system may be calculated as:

$$\bar{P}(R,t) = \frac{\int_A P_c(r,\theta,t)\,dA}{\int_A dA} \tag{14}$$

where dA is an element of area on the surface of the sphere and integration is performed over the required area specified by θ. The result is:

$$\frac{\bar{P}(R,t) - P_{s\infty}}{\rho} = R\frac{d^2R}{dt^2} + \frac{3}{2}\left(\frac{dR}{dt}\right)^2 + U^2\left(-\tfrac{1}{4} + \tfrac{3}{8}\cos\theta + \tfrac{3}{8}\cos^2\theta\right) + \tfrac{3}{4}U\frac{dR}{dt}(1+\cos\theta) + \tfrac{1}{4}R\frac{dU}{dt}(1+\cos\theta). \tag{15}$$

When $\theta = \pi$, we obtain:

$$\frac{\bar{P}(R,t) - P_{s\infty}}{\rho} = R\frac{d^2R}{dt^2} + \frac{3}{2}\left(\frac{dR}{dt}\right)^2 - \frac{U^2}{4}. \tag{16}$$

The condition of the continuity of stress at the boundary for a growing bubble is [29]:

$$P - \bar{P} = \frac{2\sigma}{R} + 4\mu\frac{1}{R}\frac{dR}{dt} \tag{17}$$

where P is the pressure in the bubble-droplet and is equal to the vaporization pressure of the dispersed-phase liquid. Thus:

$$\frac{P - P_{s\infty}}{\rho} = R\frac{d^2R}{dt^2} + \frac{3}{2}\left(\frac{dR}{dt}\right)^2 + \frac{2\sigma}{\rho R} + 4\mu\frac{1}{\rho R}\frac{dR}{dt} - \frac{U^2}{4}. \tag{18}$$

Re-arranging equation (18), we obtain:

$$\frac{d^2R}{dt^2} = \frac{P - P_{s\infty}}{\rho R} - \frac{3}{2R}\left(\frac{dR}{dt}\right)^2 - \frac{2\sigma}{\rho R^2} - 4\mu\frac{1}{\rho R^2}\frac{dR}{dt} + \frac{U^2}{4R}. \tag{19}$$

3.3.2. *Equation of motion of bubble-droplet system.* During the motion of a bubble-droplet system, a force due to the system acceleration and growth, may be found by integrating equation (13) over the surface of the sphere:

$$F_n = \int_{\psi=0}^{2\pi} d\psi \int_{\theta=0}^{\pi} -P_c(R,\theta,t)R^2\sin\theta\cos\theta\,d\theta \tag{20}$$

where F_n is the resultant force along the z-axis, hence:

$$F_n = \tfrac{4}{3}\pi R^3\rho g - 2\pi\rho U R^2\frac{dR}{dt} - \tfrac{2}{3}\pi\rho R^3\frac{dU}{dt}. \tag{21}$$

The first term in equation (21) is the buoyancy force and the last two terms are due to growth and acceleration of the system respectively.

Using equation (21), the Newtonian law for the bubble-droplet system can be written as:

$$m_{00}\frac{dU}{dt} = -m_{00}g + \tfrac{4}{3}\pi R^3\rho g - 2\pi\rho U R^2\frac{dR}{dt} - \tfrac{2}{3}\pi\rho R^3\frac{dU}{dt} - \frac{\pi}{2}\rho R^2U^2C_D \tag{22}$$

where m_{00} is the initial mass of the droplet and C_D is

the drag coefficient. Re-arranging equation (22), we get:

$$\frac{dU}{dt} = \frac{1}{\left(m_{00} + \frac{2\pi}{3}\rho R^3\right)}\left(-m_{00}g + \tfrac{4}{3}\pi R^3\rho g - 2\pi\rho U R^2 \frac{dR}{dt} - \frac{\pi}{2}\rho R^2 U^2 C_D\right). \quad (23)$$

3.3.3. *Energy equation.* Heat transfer to the spherical system during the interval of time dt is equal to the heat of evaporation. Hence:

$$4\pi R^2 h(T_c - T) = -h_{fg}\frac{dm}{dt} \quad (24)$$

where h is heat-transfer coefficient between the bulk of the surrounding liquid and the vaporizing layer of liquid droplet, m is the mass of unevaporated liquid, T is the boiling temperature of the evaporating liquid and T_c, the temperature of the surrounding liquid.

If h and h_{fg} are considered constant during dt, differentiation of equation (24) yields:

$$\frac{dT}{dt} = \frac{2}{R}(T_c - T)\frac{dR}{dt} + \frac{1}{4\pi}\frac{h_{fg}}{h}\frac{1}{R^2}\frac{d^2m}{dt^2}. \quad (25)$$

3.3.4. *Equation of state.* The vapour-pressure relation of the evaporating substance can be used for the determination of pressure at the existing temperature. We use the following equation [30]:

$$\log_{10} P = \frac{1}{2T}(b_0 - b_2) \quad (26)$$

where b_0 and b_2 can be calculated using the procedure in [30]. Differentiation of equation (26) yields:

$$\frac{dP}{dt} = \frac{\ln 10}{2}\frac{P}{T^2}\left[T\left(\frac{db_0}{dt} - \frac{db_2}{dt}\right) - (b_0 - b_2)\frac{dT}{dt}\right] = f\left(P, T, \frac{dT}{dt}\right). \quad (27)$$

3.3.5. *Equation of conservation of mass.* For a spherical bubble-droplet system, irrespective of the detailed geometry within the system.

$$m = \frac{m_{00} - \frac{4}{3}\pi R^3\rho_v}{1 - \frac{\rho_v}{\rho_l}}. \quad (28)$$

Neglecting changes of both ρ_l and ρ_v during dt, differentiation of equation (28) and a combination with equation (24) yields:

$$\frac{dR}{dt} = \frac{\rho_l - \rho_v}{\rho_l\rho_v h_{fg}}h(T_c - T). \quad (29)$$

Also by differentiation of equation (28) twice, we get:

$$\frac{d^2m}{dt^2} = -\frac{4\pi\rho_v\rho_l}{\rho_l - \rho_v}\left[2R\left(\frac{dR}{dt}\right)^2 + R^2\frac{d^2R}{dt^2}\right]. \quad (30)$$

3.4. *Set of equations*

Summing up, the following set of equations describes the evaporation of an ascending spherical bubble-droplet in an immiscible liquid.

$$\frac{dR}{dt} = \frac{\rho_l - \rho_v}{\rho_l\rho_v h_{fg}}h(T_c - T) \quad (29)$$

$$\frac{dZ}{dt} = U \quad (31)$$

$$\frac{d^2R}{dt^2} = \frac{P - P_{sx}}{\rho R} - \frac{3}{2R}\left(\frac{dR}{dt}\right)^2 - \frac{2\sigma}{\rho R^2} - 4\mu\frac{1}{\rho R^2}\frac{dR}{dt} + \frac{U^2}{4R} \quad (19)$$

$$\frac{dU}{dt} = \frac{1}{(m_{00} + \frac{2}{3}\pi\rho R^3)}\left(-m_{00}g + \tfrac{4}{3}\pi R^3\rho g - 2\pi\rho U R^2\frac{dR}{dt} - \frac{\pi}{2}\rho R^2 U^2 C_D\right) \quad (23)$$

$$\frac{dT}{dt} = \frac{2}{R}(T_c - T)\frac{dR}{dt} + \frac{1}{4\pi}\frac{h_{fg}}{h}\frac{1}{R^2}\frac{d^2m}{dt^2} \quad (25)$$

$$\frac{dP}{dt} = f\left(P, T, \frac{dT}{dt}\right) \quad (27)$$

and

$$\frac{d^2m}{dt^2} = -\frac{4\pi\rho_v\rho_l}{\rho_l - \rho_v}\left[2R\left(\frac{dR}{dt}\right)^2 + R^2\frac{d^2R}{dt^2}\right]. \quad (30)$$

3.5. *Initial conditions*

All the variables in equations (19), (23), (25), (27), (29), (30) and (31) are functions of time, thus knowledge of the initial conditions is necessary. These are:

$$\left.\begin{aligned} R(0) &= R_0 \\ Z(0) &= Z_0 \\ \left(\frac{dR}{dt}\right)_{t=0} &= X_0 \\ U(0) &= U_0 \\ T(0) &= T_0 \\ P(0) &= P_0. \end{aligned}\right\} \quad (32)$$

3.6. *Solution of the governing equations*

Equations (19), (23), (25), (27), (29), (30) and (31) were solved simultaneously by a numerical method using a CDC 6400 computer machine. The values of heat-transfer coefficient h, properties of the dispersed phase (which were written as functions of temperature), drag coefficient C_D (which was written as a function of Reynolds number) were calculated at the beginning of each time step dt and were kept constant during this time.

3.7. *Additional information*

Additional information was needed for the solution of the governing equations, e.g. instantaneous heat-transfer coefficient, instantaneous drag coefficient on bubble-droplet system, interfacial tension between the vapour of the dispersed phase and the liquid of the continuous phase and the properties of both the dispersed phase and the continuous phase.

3.7.1. *Properties of the dispersed phase.* Published properties of the dispersed phase such as heat of vaporization, viscosity, thermal conductivity, densities of vapour and liquid were used. Gallent (e.g. [31–34]) reported the physical properties of hydrocarbons over a wide range of temperature. For vapour density, a method in reference [35] was used. The interfacial tension between butane vapour and water was obtained from [36]:

$$\gamma = 71.98 - 2.335P - 0.591P^2 \tag{33}$$

where γ is the interfacial tension in dyne/cm and P is the pressure in atmospheres.

We could not obtain data on the interfacial tension between the vapour of pentane and liquid water. However, analytical procedures were used. For a bubble at a liquid–liquid interface, there are three interfacial tensions present, namely, σ_{dc}, σ_{dv} and σ_{cv} where d, v, c refer to droplet, vapour, continuous phase respectively. If:

$$\sigma_{cv} > \sigma_{dv} + \sigma_{dc} \tag{34}$$

the bubble detaches from the droplet. If:

$$\sigma_{dv} > \sigma_{dc} + \sigma_{cv} \tag{35}$$

the bubble would enter into the drop. If:

$$\sigma_{dv} \leqslant \sigma_{dc} + \sigma_{cv} \tag{36}$$

and

$$\sigma_{cv} \leqslant \sigma_{dv} + \sigma_{dc} \tag{37}$$

the bubble would remain within the droplet boundary [24]. For butane, pentane/water combinations, only conditions (34) and (37) should be checked because condition (35) does not exist and condition (36) is always satisfied. For these combinations, condition (34) is not present and the bubble is known not to detach from the system. Therefore, condition (37) must be satisfied. Photographs of the three-phase interface show that σ_{cv} could be approximated to the sum of σ_{dc} and σ_{dv}. This gives the maximum value for which the bubble remains attached to the droplet.

3.7.2. *Instantaneous heat-transfer coefficient.* The heat-transfer coefficient in equation (29) is the instantaneous heat-transfer coefficient. We used the theoretical model of Sideman *et al.* [10] which is based on the instantaneous heat transfer coefficient, i.e.

$$Nu_c = 0.272(Pe_c)^{0.5}. \tag{38}$$

In [6], the instantaneous heat-transfer coefficients for pentane/distilled water combination are presented as functions of percentage evaporation (ξ) in the bubble-droplet system:

$$h = a\frac{1}{\Delta T}\frac{\xi^b}{c\xi^d + 1} \tag{39}$$

where a, b, c and d are given for different experimental conditions.

For butane/water and butane/4% and 8% sodium chloride solution combinations, the overall in-

Table 1. Initial and operating conditions and references to Figs. 2–25

Substance	Case	Initial conditions						Operating conditions		Equation number used for calculation of h	Curve number on each figure	Figure number
		$(D/d)_0$	Z_0 (m)	X_0 (m/s) $\times 10^{-3}$	U_0 (m/s) $\times 10^{-2}$	T_0 (°C)	P_0 (N/m^2)	d (m) $\times 10^{-3}$	ΔT_0 (°C)			
Butane	1	2	0.0	6.10 7.04 7.87 8.63	15.0 20.0 25.0 30.0	1.0	107233.0	1.2	2.0	38	1 2 3 4	2, 3
	2	1	0.0	6.40 6.30 6.22	8.00 8.01 8.03 [38]	0.5 1.0 1.5	105233.0 107233.0 109262.0	1.2	2.0	38	1 2 3	4
	3	1	0.0	6.30 25.67	8.01 8.17 [38]	1.0	107233.0	1.2	2.0 8.0	38	1 2	5–12
	4	2	0.0	7.04 28.4	20.0	1.0	107233.0	1.2	2.0 8.0	38	1 2	13, 14
	5	1.1	0.0	4.65 3.92	16.02 [16]	1.0	107233.0	4.0	2.0	38 40	1 2	23–25
Pentane	6	1.008	0.0	4.25 0.24	16.6 [6]	38.0	108196.0	3.6	1.6	38 40	1 2	19–22
	7	1.07	0.0	21.9 4.08	16.6 [6]	38.0	108196.0	3.2	8.0	38 40	1 2	15–18

stantaneous heat-transfer coefficient is given by Simpson *et al.* [18] as:

$$\bar{h}_0 = \frac{2.57(D/d)^{1/6}}{1+0.206(D/d)^{5/12}}. \quad (40)$$

Equation (40) has been obtained using experimental data for single butane droplets about 3.75 mm dia and temperature driving force ΔT, 1.5°C–8.0°C which gives the value of the heat-transfer coefficient to within $\pm 18\%$ up to 90% evaporation of the liquid butane.

3.7.3. *Drag coefficient.* The drag coefficient in equation (23) is the instantaneous drag coefficient of a bubble-droplet rising in an immiscible liquid. Due to lack of data on drag coefficients for a moving bubble-droplet, we have chosen to use available data on the motion of gas bubbles in liquids [37].

4. RESULTS

Seven cases are considered for two combinations – butane/distilled water and pentane/distilled water respectively (see Table 1).

The importance of initial droplet size, initial velocity and initial temperature was examined by solving the set of equations, assuming different values for each initial condition, while maintaining the others the same, except for the initial droplet size, in which the initial velocity was to be changed accordingly. Initial growth rate was calculated from equation (29) using heat-transfer coefficient from equation (38). We found that longer evaporation time is needed for larger droplets. The final level of the bubble and the vaporization temperature drop during the rise of the bubble-droplet is higher for the larger droplets. It is useful to find the effect of the initial velocity because of the expected experimental error often encountered in determining the initial velocity. The effect is apparent only in the early stages of evaporation and then the velocities coincide in the latter stages of evaporation, Fig. 2 (Case 1, Table 1). Consequently, heat-transfer coefficients are different in the early stages. The growth rate values are smaller for the lower velocities, Fig. 3. It is found that the effect of the initial velocity on total evaporation time is insignificant. The total evaporation time and the temperature drop during the bubble-droplet rise is not significantly affected by the initial droplet temperature, Fig. 4 (Case 2, Table 1).

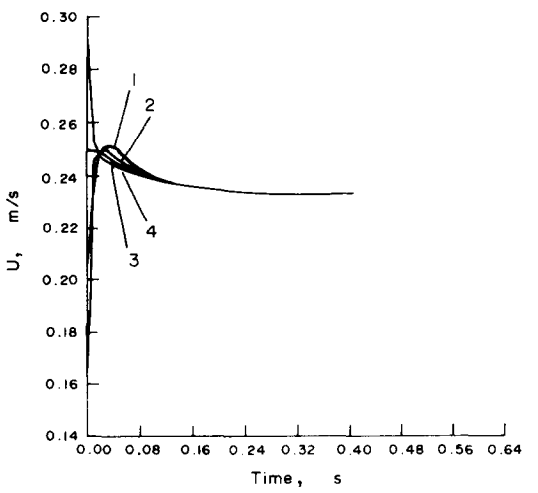

FIG. 2. Rise velocity vs time.

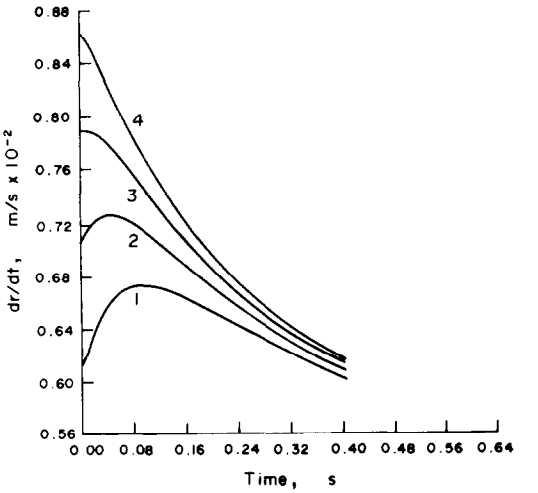

FIG. 3. Growth rate vs time.

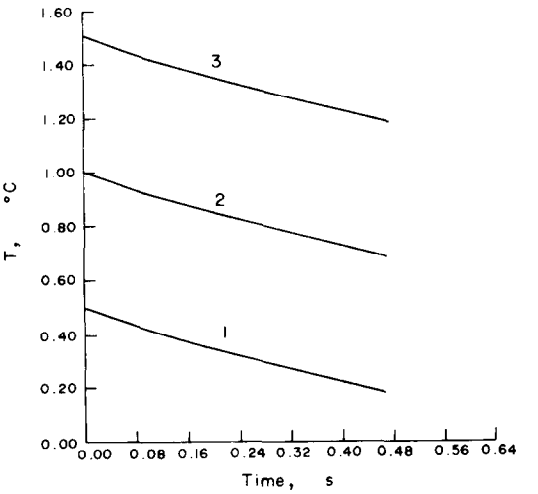

FIG. 4. Temperature vs time.

Some results of Case 3 are given in Figs. 5–7 which show the rate of change of diameter ratio, volume and growth rate vs time respectively. Equation (38) is used for the determination of heat-transfer coefficient. As can be seen from equation (29), the growth rate is directly proportional to the heat-transfer coefficient. Values of heat-transfer coefficients are shown in Fig. 8.

In equation (38), the heat-transfer coefficient is a function of Reynolds number and hence the effect of velocity is apparent. Rise velocity of the bubble-droplet is shown in Fig. 9. The decrease and then increase of velocity (Curve 2) caused a decrease and

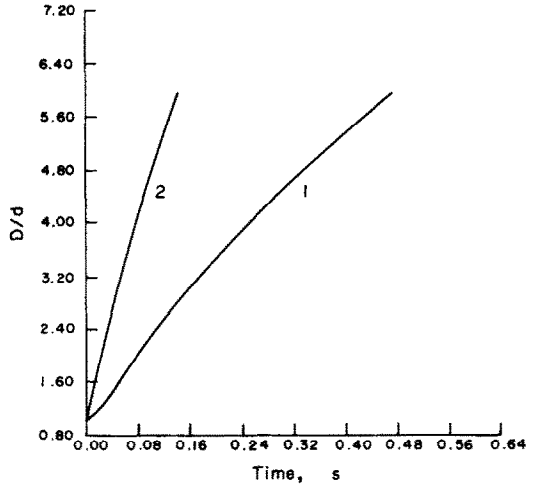

FIG. 5. Diameter ratio vs time.

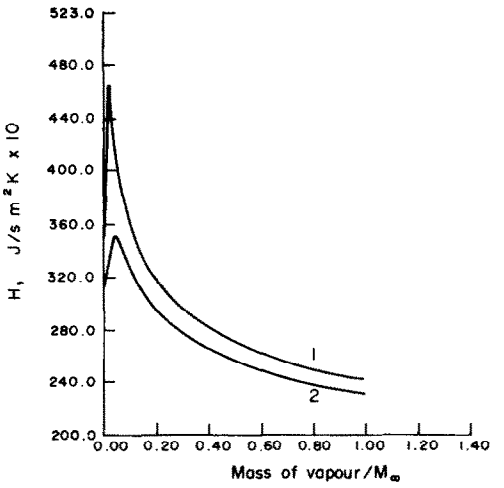

FIG. 8. Heat-transfer coefficient vs mass ratio.

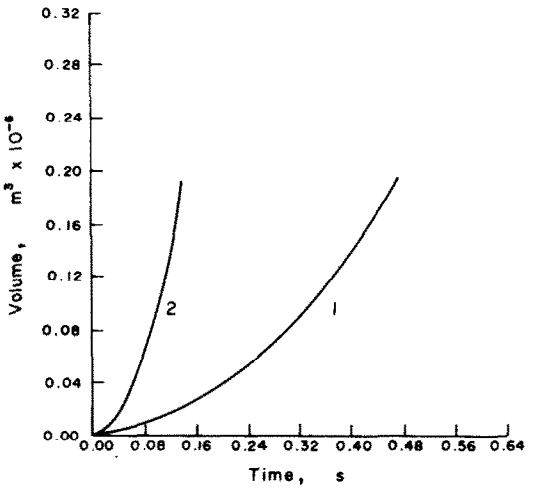

FIG. 6. Volume vs time.

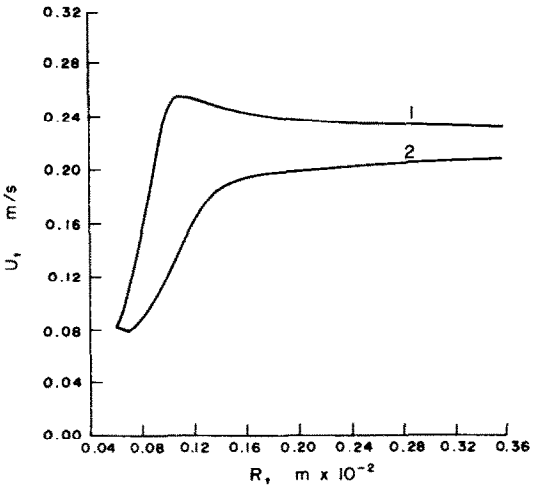

FIG. 9. Rise velocity vs radius.

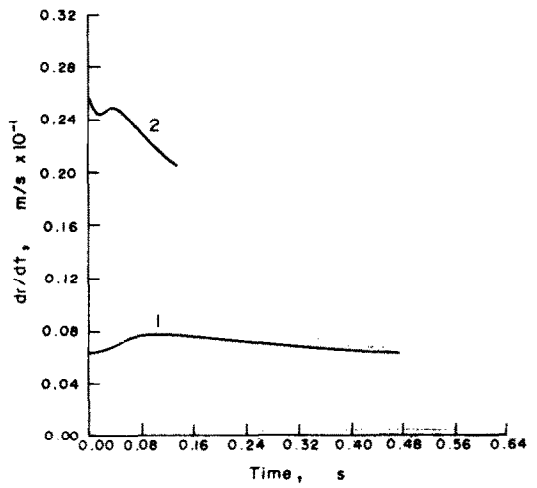

FIG. 7. Growth rate vs time.

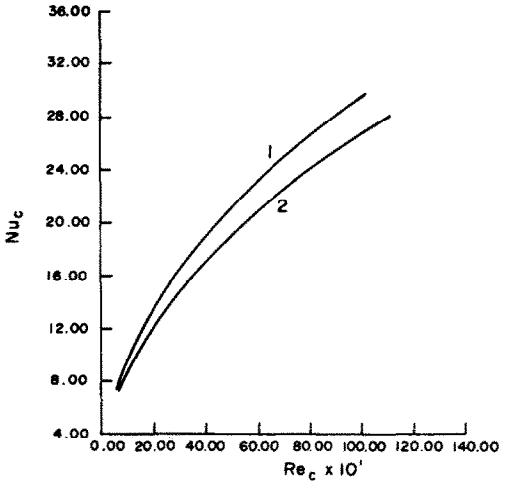

FIG. 10. Nusselt number vs Reynolds number.

then an increase of heat-transfer coefficient, Fig. 8. The initial decrease of velocity could be due to higher values of dR/dt which from equation (23) causes a resisting force against the motion of the bubble-droplet system. This behaviour does not occur when $\Delta T = 2°C$ than when $\Delta T = 8°C$ because of lower values of dR/dt in the former case (Curve 1, Fig. 7). In Fig. 10, Nusselt number is plotted against

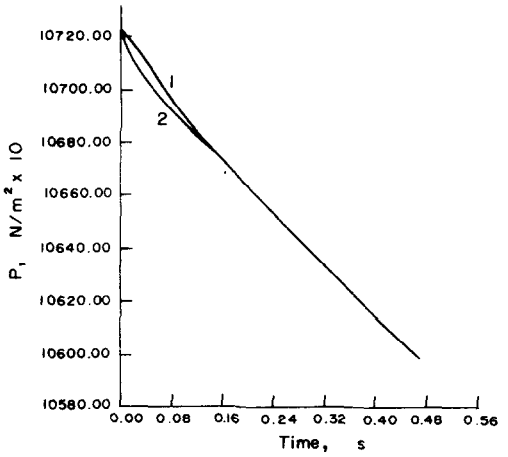

FIG. 11. Pressure vs time.

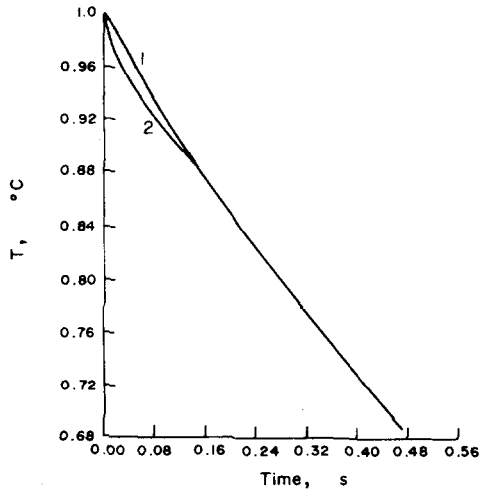

FIG. 12. Temperature vs time.

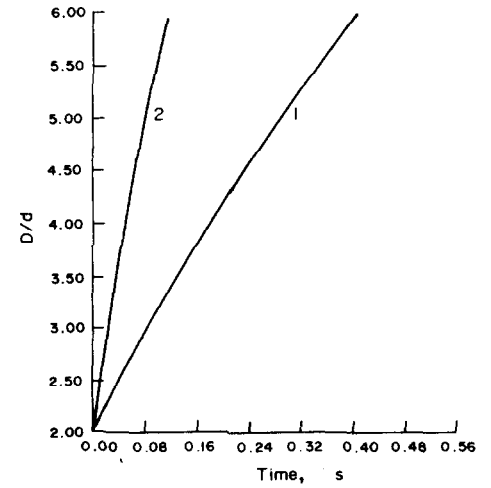

FIG. 13. Diameter ratio vs time.

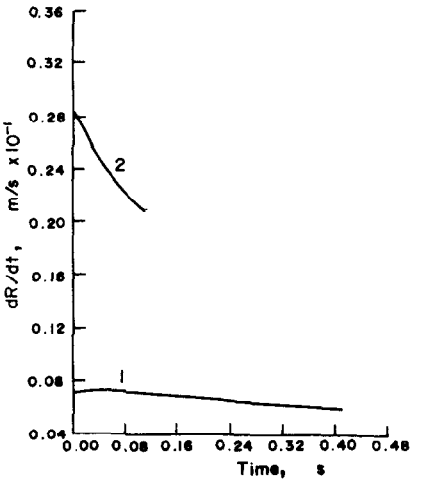

FIG. 14. Growth rate vs time.

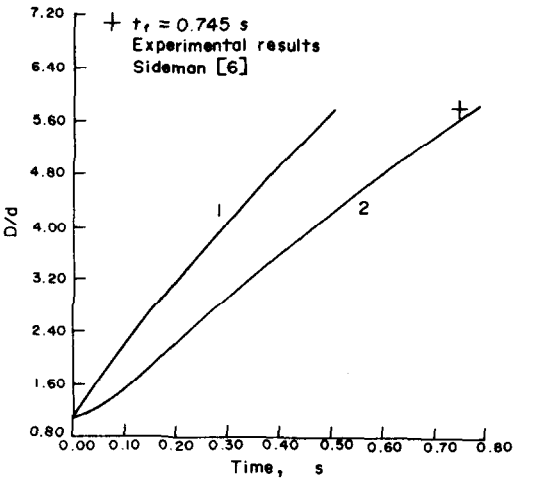

FIG. 15. Diameter ratio vs time.

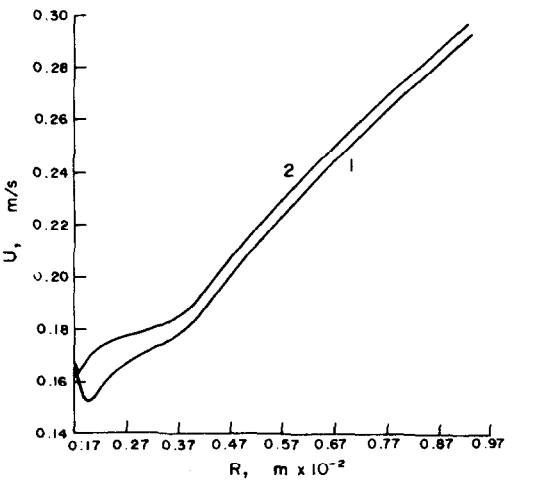

FIG. 16. Rise velocity vs radius.

Reynolds number. In Figs. 11 and 12, the decrease of vaporization pressure and temperature are shown vs time respectively. In Case 4, at $t = 0$, the diameter ratio has already reached 2 and the percentage of evaporation at this stage was 3.3%. Some of the results for this case are given in Figs. 13 and 14.

For pentane/distilled water combination (Cases 6 and 7, Table 1), heat-transfer coefficients are obtained from equations (38) and (39). Results are shown in Figs. 15–22. From Figs. 17 and 20 we can see that up to about 5% evaporation, applying Sideman's experimental results showed an increase

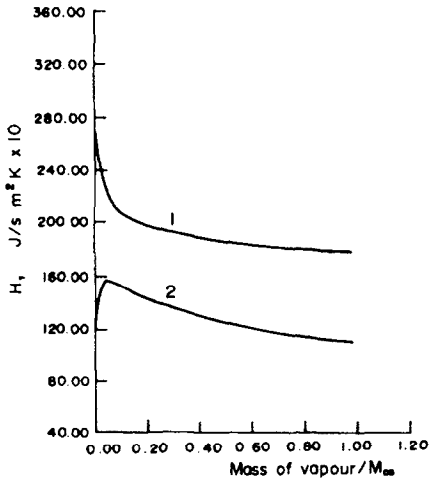

FIG. 17. Heat-transfer coefficient vs mass ratio.

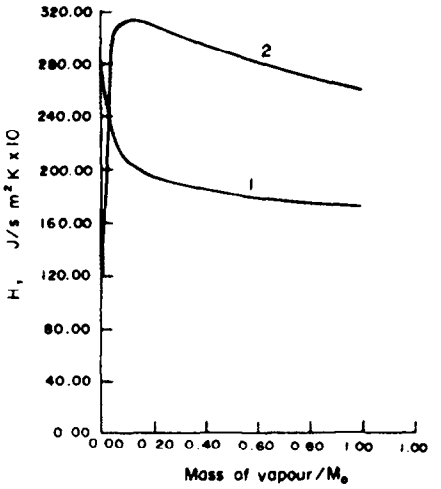

FIG. 20. Heat-transfer coefficient vs mass ratio.

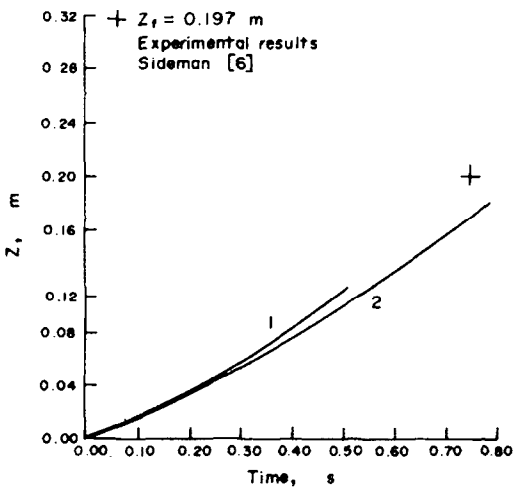

FIG. 18. Height vs time.

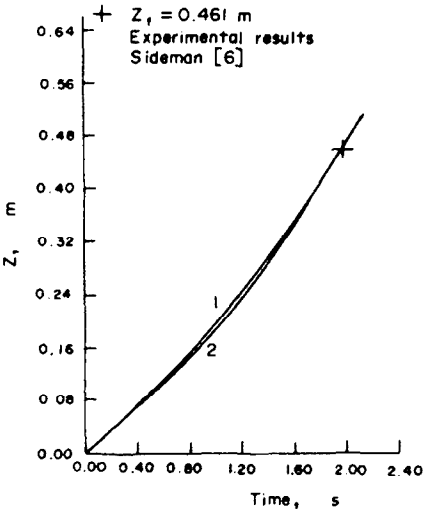

FIG. 21. Height vs time.

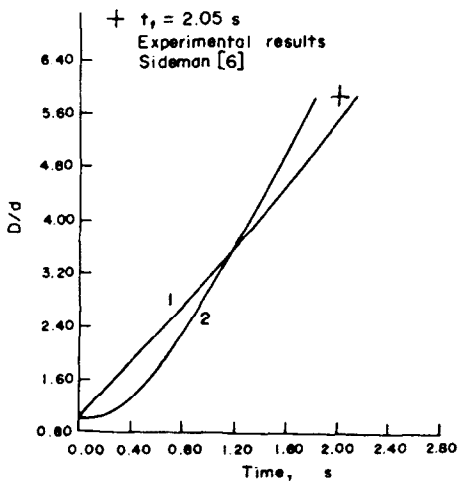

FIG. 19. Diameter ratio vs time.

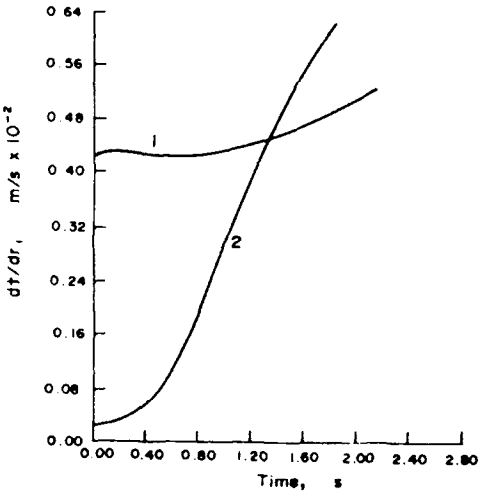

FIG. 22. Growth rate vs time.

(Curve 2), while application of his model (Curve 1) resulted in decreasing the heat-transfer coefficients. At higher percentage of evaporation, there is a gradual decrease of heat-transfer coefficients. Higher values are obtained when $\Delta T = 1.6°C$ (Fig. 20) than when $\Delta T = 8°C$ (Fig. 17).

5. DISCUSSION AND COMPARISON OF THE THEORETICAL RESULTS WITH EXPERIMENT

The governing equations (19), (23), (25), (27), (29), (30) and (31) describe a growing and accelerating spherical boundary. Depending on the initial size of the droplet, the change from spherical shape can

occur either in the early stages of evaporation or in later stages. For a pentane droplet 3.5 mm dia evaporating in water, the shape of the bubble-droplet appeared not to be spherical when about 10% evaporation is reached [6]. Its equivalent spherical diameter at this stage is about 10 mm. An air bubble of 10 mm dia rising in water has a spherical cap shape [39]. A pentane droplet with an initial diameter of 1.2 mm is transformed into a bubble of about 7 mm dia when its liquid content is fully evaporated. The bubble dimensions are within the range where the shape changes from oblate spheroid to spherical cap. Since in the introduced model, the boundary conditions are those of growing spherical bubbles and the pressure distribution at the bubble boundary is integrated over the entire surface of the sphere, therefore this model is more accurate when most of the bubble-droplet system is occupied with vapour which is expected to happen at about 1% evaporation. Thus, we may conclude that the spherical assumption can be applied to droplets of relatively small size (e.g. less than 1.2 mm dia) from about 1–100% of evaporation and for droplets of relatively large size (about 3.5 mm dia), from about 1–10% evaporation. In this range, the model is expected to give reasonable results.

Comparison of the theoretical result with experiment are made for Cases 5, 6 and 7 (Table 1). Heat-transfer coefficient for Case 5 is obtained from equations (38) and (40) and for Cases 6 and 7, from equations (38) and (39). Experimental results for Case 5 (butane/water combination) are given in [16] [Table 1(*g*)] and for Cases 6 and 7 (pentane/distilled water combination) in [6] (Table 1, Runs 1 and 14 respectively).

From Fig. 19 for a pentane drop 3.6 mm dia and a temperature difference $\Delta T = 1.6°C$, the total evaporation time obtained by Sideman [6] is 2.05 s. The time predicted by the present model is 2.15 s (when the heat-transfer coefficient is obtained from Sideman's theoretical model) and 1.83 s (when heat-transfer coefficient is obtained from his experimental correlation). From Fig. 21, the height for complete evaporation as obtained experimentally by Sideman [6] is 0.461 m, while the height as predicted by the present model is 0.413 and 0.514 m respectively. For $\Delta T = 8°C$, comparisons are made in Figs. 15 and 18.

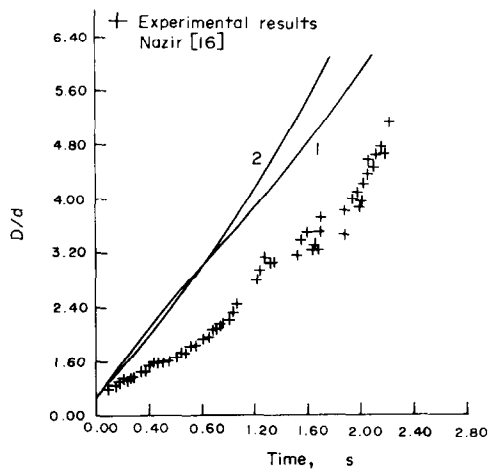

FIG. 23. Diameter ratio vs time.

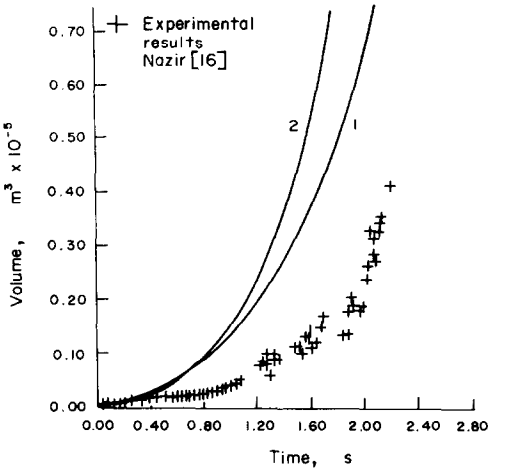

FIG. 24. Volume vs time.

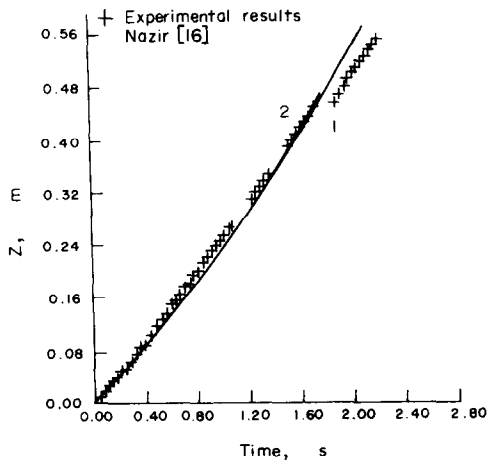

FIG. 25. Height vs time.

Figures 15–21 show that when $\Delta T = 1.6°C$, the results of application of the theoretical model and experimental results of Sideman to the present model agree better than when $\Delta T = 8°C$.

The results for Case 5 (Figs. 23–25) show that the trend of the curves predicted by this model is correct but the predicted total evaporation time is shorter than the time obtained experimentally.

CONCLUSIONS

A theoretical model of an evaporating droplet in an immiscible liquid was presented. This model predicts the variation of bubble-droplet radius, height, velocity, temperature and pressure against time. Consequently, the total evaporation time and the travelled distance for the complete evaporation are obtained. A comparison between the results predicted by the model and the available experimental data shows good agreement.

In the considered range, the results show that the initial velocity and initial temperature are not decisive factors.

Results obtained using Sideman's theoretical model showed rather high values of heat-transfer coefficients at the early stages of evaporation. However, Sideman's model can be used in conjunction with this model for the study of parameters involved.

REFERENCES

1. K. S. Spiegler, *Principles of Desalination.* Academic Press, New York (1966).
2. E. D. Howe, *Fundamentals of Water Desalination.* Marcel Dekker, New York (1974).
3. J. Missirlis, Heat transfer to evaporation drops, Office of Saline Water, R & D No. 658, pp. 40–43 (1971).
4. R. Nene, Heat transfer to evaporating drops, Office of Saline Water, R & D No. 823, pp. 16–20 (1972).
5. D. H. Klipstein, Heat transfer to a vaporizing immiscible drop, D.Sc. Thesis, M.I.T. (1963).
6. S. Sideman and Y. Taitel, Direct-contact heat transfer with charge of phase: Evaporation of drops in an immiscible liquid medium, *Int. J. Heat Mass Transfer* **7**, 1273–1289 (1964).
7. S. Sideman and G. Hirsh, Direct-contact heat transfer with change of phase. III. Analysis of the transfer mechanism of drops evaporating in immiscible liquid media, *Israel J. Technol.* **2**(2), 234–241 (1964).
8. S. Sideman, G. Hirsh and Y. Gat, Direct-contact heat transfer with change of phase: Effect of the initial drop size in three-phase heat exchangers, *A.I.Ch.E. Jl* **11**(6), 1081–1087 (1965).
9. S. Sideman, Direct-contact heat transfer between immiscible liquids, *Adv. Chem. Engng* **6**, 207–286 (1966).
10. S. Sideman and J. Isenberg, Direct-contact heat transfer with change of phase: Bubble growth in three-phase systems, *Desalination* **2**, 207–214 (1967).
11. C. B. Prakash and K. L. Pinder, Direct contact heat transfer between two immiscible liquids during vaporization (Part I: Measurement of heat transfer coefficient), *Can. J. Chem. Engng* **45**, 210–214 (1967).
12. C. B. Prakash and K. L. Pinder, Direct-contact heat transfer between two immiscible liquids during vaporization (Part II: Total evaporation time), *Can. J. Chem. Engng* **45**, 215–220 (1967).
13. V. N. Filatkin and A. G. Dolotov, Heat transfer during the boiling of single drops of a hydrocarbon mixture during direct contact with water (in Russian), in Tr. Vses. Nauch.-Tekh. konf. Termodin, sb. Dokl. Sekts, *Termodin Fazouykh perekhodov, potoka Neobratimykh protsessou*, pp. 321–329, Teplofiz. Svoistva Veshchestv. Leningrad. Teckhnol. Inst. Khlod. prom.: Leningrad, USSR (1970).
14. A. E. S. Adams and K. L. Pinder, Average heat transfer coefficient during the direct evaporation of a liquid drop, *Can. J. Chem. Engng* **50**, 707–713 (1972).
15. A. Selecki and L. Gradon, Über den Verdampfungs mechanismus eines sich in einer nicht mischbaren Flüssigkeit bewegenden Flüssigkeitstropfens (in German), *Chemie-Ingr-Tech.* **44**(18), 1077–1081 (1972).
16. M. Nazir, Direct contact heat transfer, evaporation of butane drops in brine, Ph.D. Thesis, Univ. of Strathclyde, Glasgow (1972).
17. H. C. Simpson, G. C. Beggs and M. Nazir, Evaporation of butane drops in brine, *Desalination* **15**, 11–23 (1974).
18. H. C. Simpson, G. C. Beggs and M. Nazir, Evaporation of a droplet of one liquid rising through a second immiscible liquid. A new theory of the heat transfer process, in *Heat Transfer, Proc. 5th Int. Heat Transfer Conf.*, Vol. 5, pp. 59–63 (1974).
19. Y. Tochitani, Y. H. Mori and K. Komotori, Vaporization of a liquid injected into an immiscible liquid through a single nozzle, *Wärme- und Stoffübertragung* **8**, 249–259 (1975).
20. A. Selecki and L. Gradon, Equation of motion of an expanding vapour drop in an immiscible liquid medium, *Int. J. Heat Mass Transfer* **19**, 925–929 (1976).
21. L. Gradon and A. Selecki, Evaporation of a liquid drop immersed in another immiscible liquid. The case of $\sigma_c < \sigma_d$, *Int. J. Heat Mass Transfer* **20**, 459–466 (1977).
22. Y. Tochitani, Y. H. Mori and K. Komotori, Vaporization of single liquid drops in an immiscible liquid. Part 1: Forms and motions of vaporizing drops, *Wärme- und Stoffübertragung* **10**, 51–59 (1977).
23. Y. Tochitani, Y. H. Mori and K. Komotori, Vaporization of single liquid drops in an immiscible liquid. Part 2: Heat transfer characteristics, *Wärme- und Stoffübertragung* **10**, 71–79 (1977).
24. G. R. Moore, Vaporization of superheated drops in liquids, *A.I.Ch.E. Jl* **5**(4), 458–466 (1959).
25. T. J. Jarvis, M. D. Donohue and J. L. Katz, Bubble nucleation mechanisms of liquid droplets superheated in other liquids, *J. Colloid Interface Sci.* **50**(2), 359–368 (1975).
26. Y. H. Mori and K. Komotori, Boiling of single superheated drops in an immiscible liquid, *Heat Transfer – Japanese Res.* **5**, 75–95 (1976).
27. Y. H. Mori and K. Komotori, Boiling modes of volatile liquid drops in an immiscible liquid depending on degree of superheat, ASME Pub. 76-HT.13.
28. M. R. L'Ecuyer and S. N. B. Murthy, Energy transfer from a liquid to gas bubbles forming at a submerged orifice, NASA TN D-2547 (1965).
29. R. T. Knapp, *Cavitation.* McGraw-Hill, New York (1970).
30. *Engineering Sciences Data*, The evaluation of Chebyshev series used for the representation of vapour pressures, physical data, vapour pressure, Vol. 5a, Item No. PDI. Engineering Sciences Data Unit (1972).
31. R. W. Gallant, Physical properties of hydrocarbons. Part 1—Methane–Ethane–Propane–Butane, *Hydrocarb. Process.* **44**(7), 95–103 (1965).
32. R. W. Gallant, Physical properties of hydrocarbons. Part 9—Thermal conductivity of C_1 to C_4 hydrocarbons, *Hydrocarb. Process.* **45**(12), 113–121 (1966).
33. R. W. Gallant, Physical properties of hydrocarbons. Part 15—C_5–C_8 Alkanes, *Hydrocarb. Process.* **46**(7), 121–129 (1967).
34. R. W. Gallant, Physical properties of hydrocarbons. Part 17—C_4–C_5 Branched hydrocarbons, *Hydrocarb. Process.* **46**(9), 155–163 (1967).
35. *Technical Data Book*, Petroleum Refining, Density (Chapter 6). American Petroleum Institute (1970).
36. R. Massoudi and A. D. King, Jr., Effect of pressure on the surface tension of water. Adsorption of low molecular weight gases on water at 25°, *J. Phys. Chem.* **78**(22), 2262–2266 (1974).
37. W. L. Haberman and R. K. Morton, An experimental study of bubbles moving in liquids, *Trans. Am. Soc. Civ. Engrs* **121**, 227–252 (1956).
38. A. J. Klee and R. E. Treybal, Rate of rise or fall of liquid drops, *A.I.Ch.E. Jl* **2**(4), 444–447 (1956).
39. B. Rosenberg, The drag and shape of air bubbles moving in liquids, The David W. Taylor Model Basin, Report 727 (1950).

ETUDE THEORIQUE DE GOUTTES EN EVAPORATION DANS UN LIQUIDE NON MISCIBLE

Résumé—On présente une étude théorique de l'évaporation d'une goutte unique pendant son ascention dans un liquide non miscible. Les équations génériques sont établies puis résolues simultanément en utilisant une méthode numérique. Des résultats sont présentés pour deux combinaisons: butane/eau distillée et pentane/eau distillée. Le modèle est examiné pour différentes tailles initiales de gouttes, différents écarts de température et différentes vitesses et températures initiales. Les calculs sont comparés aux résultats expérimentaux antérieurs.

EINE THEORETISCHE UNTERSUCHUNG ZUR VERDAMPFUNG VON TROPFEN IN EINER NICHT MISCHBAREN FLÜSSIGKEIT

Zusammenfassung—Diese Arbeit ist eine theoretische Untersuchung über die Verdampfung eines einzelnen Tropfens, während er in einer nicht mischbaren Flüssigkeitssäule aufsteigt. Die den Vorgang bestimmenden Gleichungen werden abgeleitet und mit einer numerischen Methode simultan gelöst. Ergebnisse werden für zwei Kombinationen angegeben: Butan/destilliertes Wasser und Pentan/destilliertes Wasser. Das Modell wurde erprobt für verschiedene Anfangs-Tropfengrößen, Temperaturdifferenzen, Anfangsgeschwindigkeiten und Anfangstemperaturen. Die errechneten Ergebnisse werden mit den experimentellen Resultaten früherer Autoren verglichen.

ТЕОРЕТИЧЕСКИЙ АНАЛИЗ ИСПАРЕНИЯ КАПЕЛЬ В НЕСМЕШИВАЮЩЕЙСЯ ЖИДКОСТИ

Аннотация — В статье представлен теоретический анализ процесса испарения единичной капли во время её поднятия в столбе несмешивающейся жидкости. Полученные уравнения решены численным методом. Результаты представлены для двух сочетаний сред: бутан-дистиллированная вода и пентан-дистиллированная вода. Модель исследовалась при различных начальных размерах капель, разностях температур, начальных скоростях и начальных температурах. Результаты расчётов сопоставлены с экспериментальными данными других авторов.